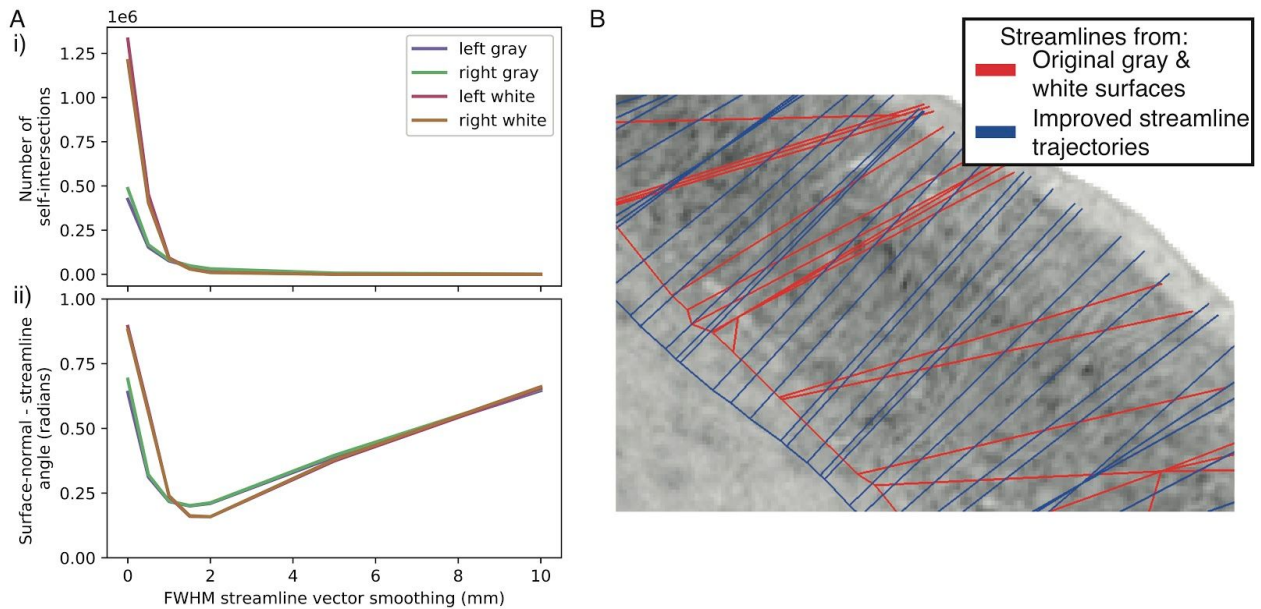
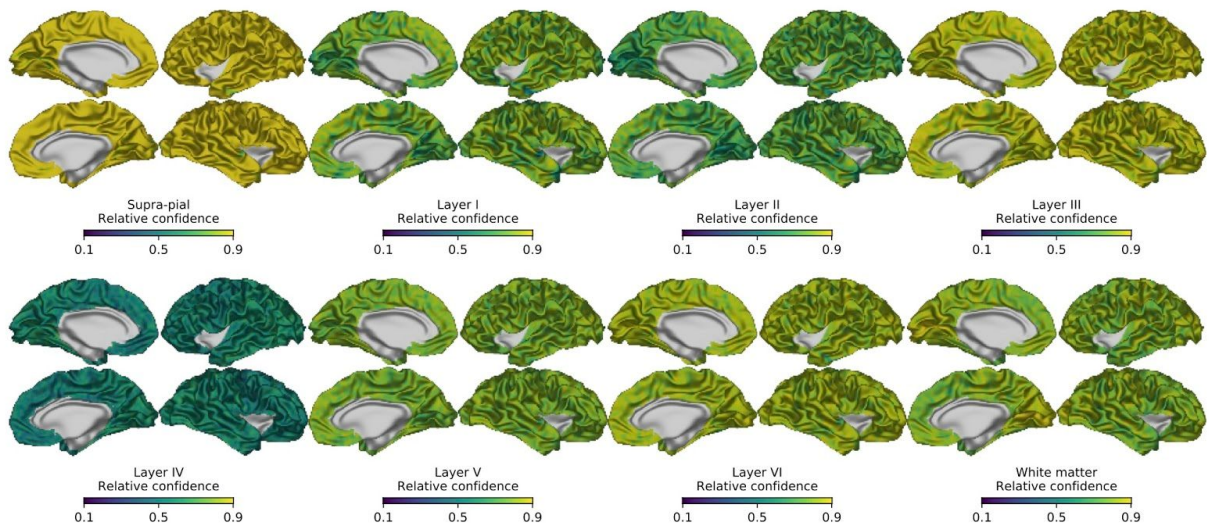


Supplementary figures:



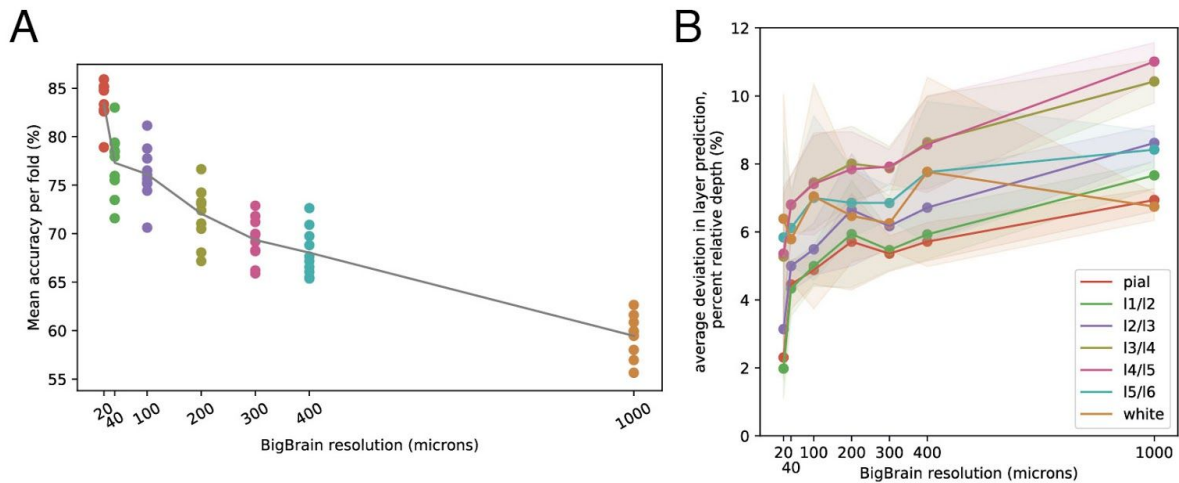
Supplementary Figure 1

Improving streamline trajectories. A) Streamline vectors were smoothed across the cortical surface by varying degrees to assess the impact of smoothing on i) the number of self intersections in the pial and white surfaces and ii) the angle between the streamline and the normal vector on the pial and white surfaces. These optimisation curves demonstrate that a FWHM of around 2mm drastically decreases the number of self-intersections and obliqueness of the streamline vectors relative to the pial and white surfaces. B) Visualising streamlines against a histological section. Streamlines more closely follow visible cortical columnar trajectories after this improvement (blue) relative to before this streamline vector smoothing process (red).



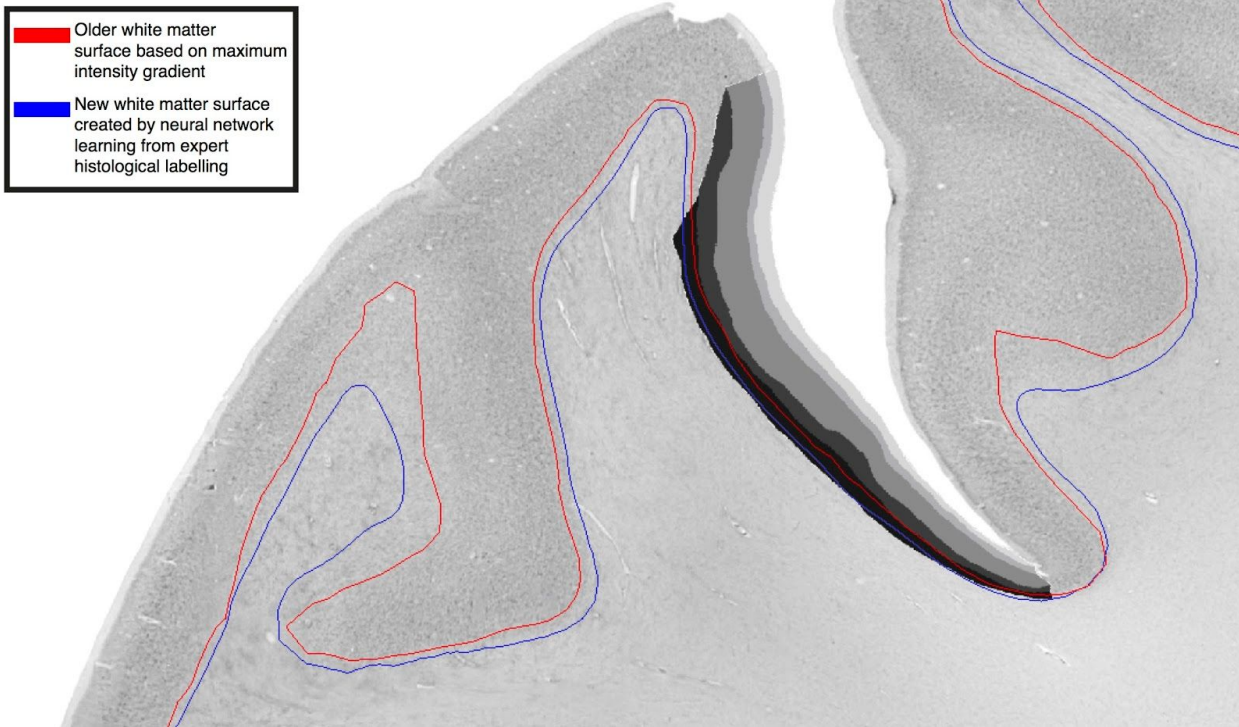
Supplementary Figure 2

Layer confidence maps. Per vertex confidence is the difference between the prediction value for the highest predicted class and the value of the 2nd highest predicted class, averaged over the whole profile. This gives an approximation of the reliability of laminar segmentations for the cortex where ground truth manual segmentations have not been carried out. Confidence for supra-pial and white matter classes was high throughout the cortex, thus increasing the confidence in overall cortical thickness measures. Layers exhibit relatively consistent confidence maps, with layer IV least confident overall. This pattern matches with visual observations that layer IV is the most difficult to identify. Regional variations in confidence can guide the choice of target regions for future extensions to the training data.



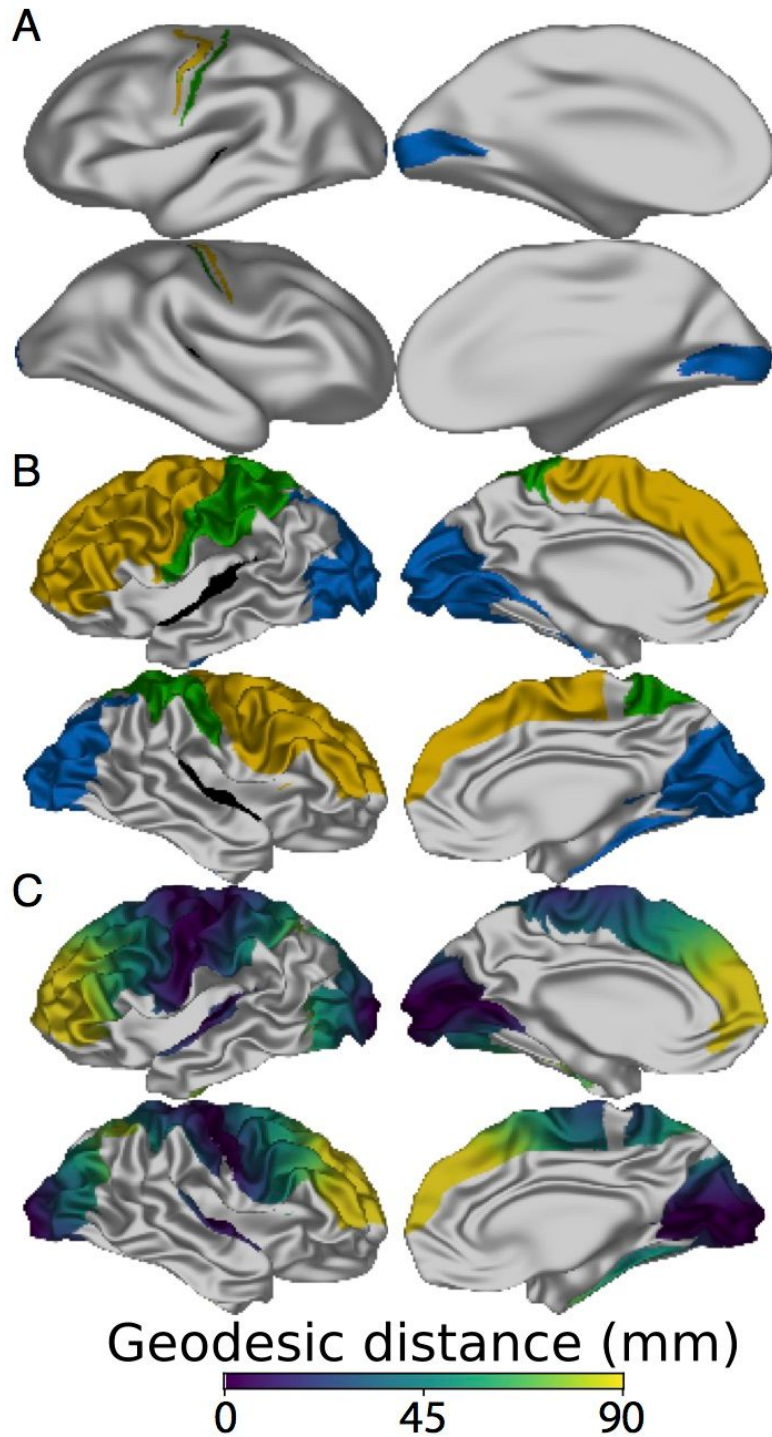
Supplementary Figure 3

Impact of voxel resolutions on overall and layer accuracies. A) Overall per-point accuracies on withheld test regions calculated using 10-fold validation. Accuracy decreases with decreasing resolution. B) Mean deviation in depth prediction on test folds between prediction and manually defined layers. Pial/layer I and layer I/II boundaries were most accurate, followed by II/III, with layer III/IV and VI/white boundaries exhibiting larger deviations



Supplementary Figure 4

Comparison of white matter surfaces generated by the neural network and by placing the white surface at the maximum intensity gradient. For visual comparison, the surfaces are overlaid on a 2D section, where manually segmented layers are available. The max intensity gradient white surface (red) was identified on lower-resolution data (200 μ m). This surface was consistently superficial to the new surface (blue), which was created based on features derived from the histological definition of the white matter surface, which is determined by the absence or presence of cortical neurons. The green surface more consistently follows the layer VIa/VIb boundary. This systematic difference highlights the role of using histological expertise when translating across scales and fields to ensure consistent definitions. It also raises an important question on the placement of the white surface in MRI cortical reconstructions which is placed at the maximum MRI intensity gradient. This gradient is determined predominantly by myelin contrast, and therefore influenced by changes interregional and longitudinal in cortical myelination. Future cortical segmentation algorithms need to be developed with closer reference to histological definitions of the gray/white boundary.



Supplementary Figure 5

A. Manually segmented primary visual (blue), primary auditory (black, partially buried in the lateral sulcus), primary somatosensory (green) and primary motor (yellow) areas, projected onto a heavily smoothed surface. B. Manually segmented regions across which cortical and laminar hierarchical thickness gradients were calculated. C. Geodesic distance across the cortical surface from the primary areas.